

Fabrication of nanoporous tungsten oxide by galvanostatic anodization

Niloy Mukherjee and Maggie Paulose

SenTech Corporation, 200 Innovation Boulevard, State College, Pennsylvania 16803

Oomman K. Varghese, G.K. Mor, and Craig A. Grimes^{a)}

Department of Electrical Engineering and Department of Materials Science and Engineering,

217 Materials Research Laboratory, The Pennsylvania State University,

University Park, Pennsylvania 16802

(Received 11 June 2003; accepted 21 July 2003)

Nanoporous tungsten oxide (WO_3), with pores of 50 to 100 nm in diameter, has been obtained by galvanostatic (constant-current) anodization of tungsten in a 0.25 M oxalic acid electrolyte. At room temperature, the optimum current density for nanoporous formation is approximately 6.5 to 8 mA/cm^2 . Monitoring of the anodization voltage during the fabrication process reveals a close match with the theoretical model of Parkhutik *et al.* [V.P. Parkhutik and V.I. Shershulsky, *J. Phys. D* **25**, 1258 (1992)] for growth of nanoporous Al_2O_3 . The as-anodized films are amorphous and crystallize upon annealing at 350 °C in an oxygen atmosphere.

Tungsten oxide (WO_3) has been receiving considerable attention in recent years for its NO_x , CO, and H_2S gas sensing properties^{1,2} as well as for use in electrochromic,^{3–10} photochromic,^{11,12} and transparent conducting electrode applications.^{13,14} To date, many different processing methods including sol-gel,^{3–5} thermal¹⁵ and e-beam⁶ evaporation, sputtering,^{15,16} spray pyrolysis,¹⁷ pulsed laser deposition,¹ colloidal chemistry,¹¹ and polymer-templating⁷ have been used to fabricate tungsten oxide thin films and nanostructures. Sun *et al.*¹¹ reported nanocrystalline WO_3 thin film preparation by a colloidal chemistry route. Both Badilescu *et al.*³ and Aliev *et al.*⁵ attempted fabrication of nanoporous WO_3 by sol-gel synthesis using nanoparticle templates; the structures obtained consisted of agglomerations of nanometer-size grains and voids ranging from 200 to 500 nm in size. Cheng *et al.*⁷ reported fabrication of WO_3 having 4–5 nm pores by block copolymer templating. Despite a less than optimum nanoporous structure in some of the above cases, these studies have reported enhanced electrochromic properties, with high coloration densities and higher

rates for coloring and bleaching.^{3,5,7} For photochromic applications, nanometer grain sizes result in a blue shift of the absorption peaks.¹¹

Our interest is in developing a low cost, relatively simple route of fabricating nanoporous tungsten oxide based on anodization. In addition to the promise of nanoporous WO_3 for greatly enhancing electro- and photochromic properties, earlier work of the authors has shown that nanostructured Al_2O_3 and TiO_2 made by anodization display significantly enhanced gas sensing properties compared to their bulk counterparts.^{18–20} Though anodization has been used in the past to fabricate tungsten oxide, the resulting films were not nanoporous.^{21–23} Specific routes for nanostructure fabrication by anodization have not, to our knowledge, yet been reported.

We report herein the fabrication of nanoporous tungsten oxide by the process of anodization. Pure tungsten foil (99.95%) of 0.25-mm thickness was obtained from Alfa Aesar (Ward Hill, MA). Prior to anodization, the metal samples were cleaned by immersion in an acetone ultrasonic bath for 10 min, followed by a deionized water rinse, then allowed to dry in air. Anodization was performed in oxalic acid by the galvanostatic (constant-current) method at room temperature without electrolyte stirring. Optimal nanoporous results were obtained from

^{a)}e-mail: cgrimes@enr.psu.edu

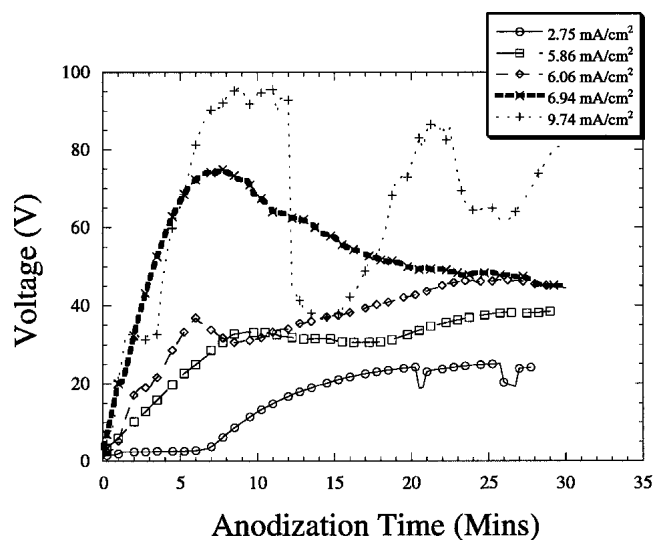


FIG. 1. Plot showing the variation in voltage during constant-current anodization of pure tungsten foils in 0.25 M oxalic acid at varying current densities.

a solution of 0.25 M oxalic acid in deionized water. Constant current was applied by means of a direct current (dc) power source, and the time-dependent behavior of the voltage was recorded.

Figure 1 shows the voltage versus time behavior of the anodization for a range of different current densities (total current divided by anode surface area). As seen, at a current density of 2.75 mA/cm² the voltage increases slowly in the beginning, goes through a region of higher slope, and then saturates. At current densities of 5.86 mA/cm² and 6.06 mA/cm², the initial voltage-time slope is larger, with the voltage peaking after approximately 5 to 10 min, after which it decreases and then eventually increases again at a slower rate. At current density of 6.94 mA/cm², the voltage is seen to peak in approximately 7 min and thereafter falls at a steadily decreasing rate, approaching a constant value after 30 min. At the highest current density tested, 9.74 mA/cm², the voltage is seen to exhibit a cyclic behavior.

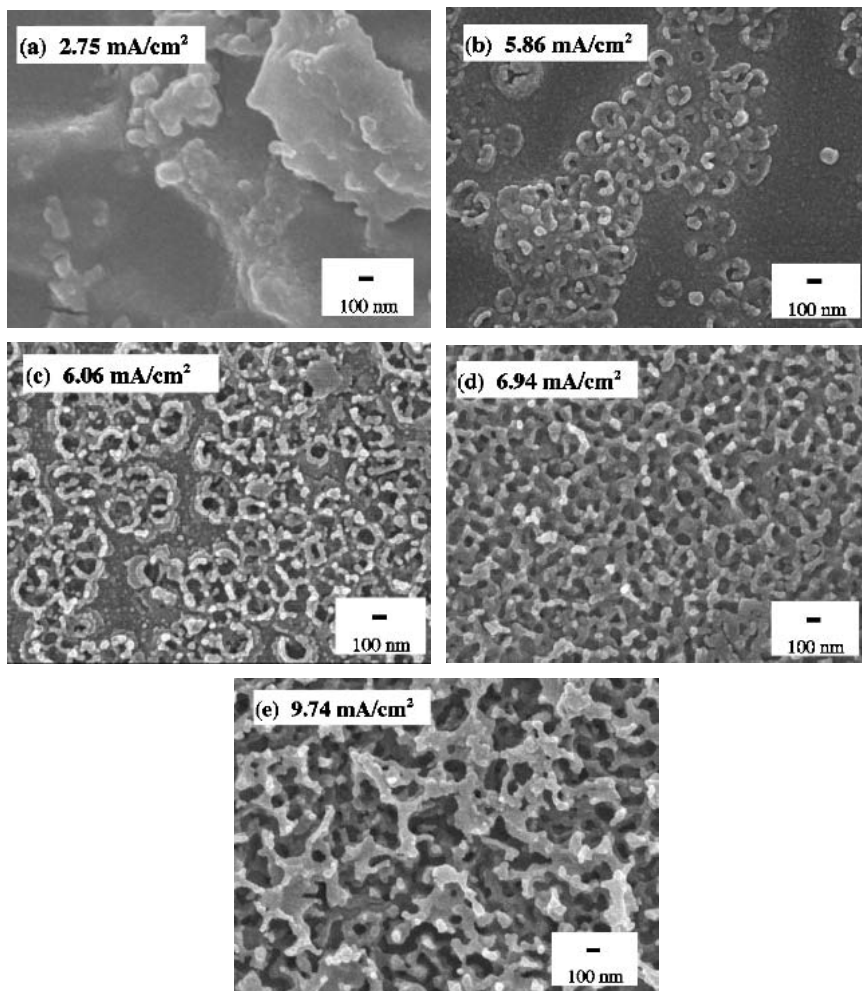


FIG. 2. A series of micrographs obtained after 30 min anodization at different current densities (see Fig. 1). Study shows the evolution of the nanoporous structure as a function of current density: (a) 2.75 mA/cm², (b) 5.86 mA/cm², (c) 6.06 mA/cm², (d) 6.94 mA/cm², and (e) 9.74 mA/cm².

The results of Fig. 1 can be correlated with scanning electron microscopy observations. Figure 2 shows a series of five images (JEOL 6700 FE-SEM, Peabody, MA), all taken at the same magnification of 50,000 \times , corresponding to the samples whose voltage behavior is presented in Fig. 1 and representing the structure of the anodized film at the end of 30-min anodization. As seen in Fig. 2(a), the 2.75 mA/cm² sample has a uniform surface film with no porosity visible. A porous structure is seen to cover parts of the 5.86 mA/cm² sample, Fig. 2(b). The area covered by the porous structure has increased substantially in the case of the 6.06 mA/cm² sample, Fig. 2(c), and a completely nanoporous structure is obtained in the case of the 6.94 mA/cm² sample, as seen in Fig. 2(d). The pore sizes in Figs. 2(a)–2(d) are in the 50–100-nm range. The structure obtained from the 9.74 mA/cm² sample, Fig. 2(e), is also porous, but the average pore size is significantly greater than 100 nm. The thickness of the resulting oxide layer, in all cases, is approximately 150 nm.

Comparing Figs. 1 and 2, we find that a nanoporous structure is obtained only in the cases where the voltage first peaks and then decreases, in agreement with the theory of Parkhutik *et al.*²⁴ developed for understanding the kinetics of porous aluminum oxide formation during anodization. An increasing anodization voltage indicates progressive formation of surface oxide film. A decreasing anodization voltage after an initial peak indicates pore formation by field-induced oxide dissolution at points where pores initially nucleate. As the pores deepen, the thickness of the barrier layer decreases, and the voltage needed to drive the same current decreases correspondingly. For particular values of applied current density and barrier layer thickness, given that other experimental conditions remain constant, the rates of oxidation and dissolution can balance each other exactly and a steady-state can eventually be reached with barrier layer thickness and voltage remaining constant with time thereafter. In the results presented above, the current density of 6.94 mA/cm² is closest to such a steady-state condition. In the 2.75 mA/cm² sample, the current density is too low to cause pore nucleation. As the current density is increased, pore formation begins, and the fraction of the total surface covered by the nanoporous structure at the end of 30 min anodization gradually increases, Figs. 2(b) and 2(c), and eventually the entire film becomes nanoporous as seen in Fig. 2(d). For current densities higher than this range, the system cycles back and forth with oxidation and dissolution being alternately dominant as a function of time. Thus, though a porous structure is seen in the case of the 9.74 mA/cm² sample, Fig. 2(e), the structure is quite rough due to the fluctuating voltage. Further experiments have shown that the processing window for nanostructure formation extends from 6.5 mA/cm² up to 8 mA/cm². It should be noted that

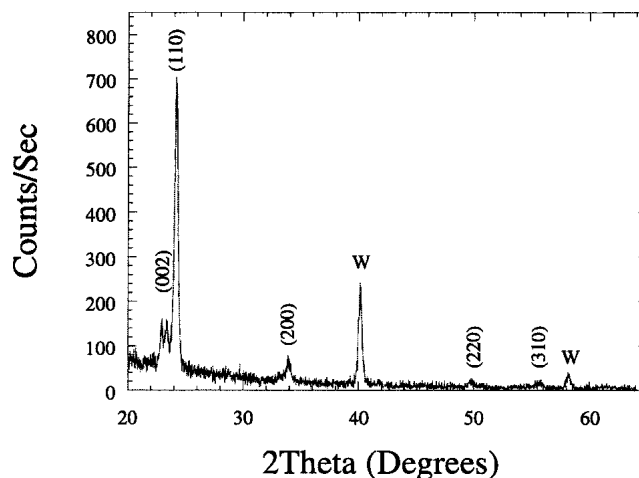


FIG. 3. GAXRD pattern obtained from nanoporous tungsten oxide after annealing at 350 °C for 3 h in a pure O₂ atmosphere. The crystalline nature of the annealed film is clearly evident. Indexed peaks correspond to those of monoclinic WO₃ while “W” denotes substrate. The as-anodized film is amorphous.

this processing window is most likely dependent on the metallurgical quality of the starting metal foil. Similar anodization experiments have been conducted using a 0.5 M oxalic acid electrolyte, in which case the processing window for obtaining the nanoporous structure was centered on a current density of approximately 5 mA/cm² with the resulting pores being 100–200-nm in size.

Glancing angle x-ray diffraction (GAXRD) was performed on the anodized film to evaluate crystallinity. The as-anodized material proved to be amorphous. To induce crystallization, the samples were annealed at 350 °C in pure O₂ ambient for 3 h with heating and cooling rates of 3 °C/min. The GAXRD pattern from an annealed film is shown in Fig. 3. The pattern shows that the sample has crystallized with annealing; the peaks have been indexed as per the monoclinic WO₃ structure, with peaks arising from the tungsten substrate labeled “W.”

In conclusion, nanoporous tungsten oxide has been obtained by galvanostatic anodization in oxalic acid. The structure is more regular and the pore size range is smaller than that reported from most sol-gel synthesis studies. Anodization offers a simple, efficient, and inexpensive way to obtain and control WO₃ nanoporous structures. This type of regular and homogeneous nanoporous structure offers an opportunity for enhancing the gas sensitivities as well as the electro- and photochromic properties of this technologically important material.

ACKNOWLEDGMENTS

This work was partially supported by NASA under Grant No. NAG-1-01036 and by a seed grant provided by Penn State Materials Research Institute and the Penn State Materials Research Science and Engineering Center (MRSEC) under National Science Foundation (NSF) Grant Nos. DMR 0080019 and DMR 0213623.

REFERENCES

1. H. Kawasaki, J. Namba, K. Iwatsuji, Y. Suda, K. Wada, K. Ebihara, and T. Ohshima, *Appl. Surf. Sci.* **41**, 547 (2002).
2. W. Gopel and K.D. Schierbaum, *Sens. Actuators B* **26–27**, 1 (1995).
3. S. Badilescu and P.V. Ashrit, *Solid State Ionics* **158**, 187 (2003).
4. E. Ozkan, S.H. Lee, P. Liu, C.E. Tracy, F.Z. Tepehan, J.R. Pitts, and S.K. Deb, *Solid State Ionics* **149**, 139 (2002).
5. A.E. Aliev and H.W. Shin, *Solid State Ionics* **154–155**, 425 (2002).
6. A. Antonaia, M.L. Addonizio, C. Minarini, T. Polichetti, and M. Vittori-Antisari, *Electrochim. Acta* **46**, 2221 (2001).
7. W. Cheng, E. Baudrin, B. Dunn, and J.I. Zink, *J. Mater. Chem.* **11**, 92 (2001).
8. C.G. Granqvist, *Electrochim. Acta* **44**, 3005 (1999).
9. R.D. Rauh, *Electrochim. Acta* **44**, 3165 (1999).
10. S.H. Lee, H.M. Cheong, J.G. Zhang, A. Mascarenhas, D.K. Benson, and S.K. Deb, *Appl. Phys. Lett.* **74**, 242 (1999).
11. M. Sun, N. Xu, Y.W. Cao, J.N. Yao, and E.G. Wang, *J. Mater. Res.* **15**, 927 (2000).
12. A.I. Gavrilyuk, *Electrochim. Acta* **44**, 3027 (1999).
13. T.J. Coutts, X. Li, and T.A. Cessert, *IEEE Electron. Lett.* **26**, 660 (1990).
14. B. Stierna and C.G. Granqvist, *Appl. Opt.* **29**, 117 (1991).
15. S.H. Lee, H.M. Cheong, C.E. Tracy, A. Mascarenhas, D.K. Benson, and S.K. Deb, *Electrochim. Acta* **44**, 3111 (1999).
16. Y. Nagasawa, K. Tabata, and H. Ohnishi, *Appl. Surf. Sci.* **121–122**, 327 (1997).
17. T. Brousse and D.M. Schleich, *Sens. Actuators B* **31**, 77 (1996).
18. O.K. Varghese, D. Gong, M. Paulose, C.A. Grimes, and E.C. Dickey, *J. Mater. Res.* **17**, 1162 (2002).
19. O.K. Varghese, C.A. Grimes, M. Paulose, K.G. Ong, and E.C. Dickey, *Adv. Mater.* **15**, 624 (2003).
20. O.K. Varghese and C.A. Grimes, *J. of Nanoscience and Nanotechnology* (in press).
21. F. Di Quarto, A. Di Paola, and C. Sunseri, *Electrochim. Acta* **26**, 1177 (1981).
22. D.J. Beckstead, G.M. Pepin, and J.L. Ord, *J. Electrochem. Soc.* **136**, 362 (1989).
23. J.L. Ord and D.J. De Smet, *J. Electrochem. Soc.* **139**, 359 (1992).
24. V.P. Parkhutik and V.I. Shershulsky, *J. Phys. D: Appl. Phys.* **25**, 1258 (1992).